Computational Performance Analysis of the Perforated and Flat Plates Double Pass Solar Air Heaters

P. P. Dutta, P. Goswami, A. Sharma, Polash P. Dutta, and M. G. Baruah

Nomenclature

A	Area (m^2)
a	Length of specimen (m)
D_h	Hydraulic diameter of SAH (m)
FVM	Finite volume method
f	Coefficient of friction
h	Heat transfer coefficient (W/m^{2}K)
k	Thermal conductivity (W/mK)
Nu	Nusselt number
ΔP	Pressure drop (Pa)
Pr	Prandtl number
R_e	Reynolds number
SAH	Solar air heater
u, v, w	Velocity components in X, Y, Z axes

Greek Symbols

α	Volume fraction (dimensionless)
η	Efficiency (dimensionless)
ρ	Density of air (kg/m^3)
μ	Coefficient of viscosity (kg/ms)
δ	Delta

P. P. Dutta (✉) · A. Sharma · P. P. Dutta · M. G. Baruah
Department of Mechanical Engineering, Tezpur University, Napaam, Sonitpur, India

P. Goswami
Indian Institute of Technology, Kharagpur, India

σ Diffusion Prandtl number
ε Dissipation kinetic energy, m^2/s^3

Superscripts

(n)   nth iteration

Subscripts

a   Air

1 Introduction

The natural non-renewable energy resources are diminishing each day due to the ever increasing population and industrialization. During 1970, solar energy was considered as one of the finest alternatives for fulfilling the snowballing demand for energy in the world. As a result of intensification in oil prices in the 1970s, a committed and sustainable research work was supported for extraction of maximum benefit from the solar energy [1]. Of all the renewable energy sources available, solar energy has the paramount reliability and sustainability. It has the potential to cope with the current energy demand to a considerable extent. As the solar energy radiation is elevated to a higher temperature than the ambient air, it may be utilized in a more beneficial ways [2]. A good part of Indian terrain is positioned in the tropical region of the globe and it has a decent hand access to the solar energy. Therefore, this territory of India receives a fair amount solar insolation. As a result, it is an ideal place for generating useful heat and electricity from solar potential. India's location on globe is fortunate enough to receive solar energy equivalent of more than 5000 trillion kWh per year. This is much more than the total annual consumption by the population. The daily global radiation is around 5 kWh per square meter per day with sunshine ranging between 2300 and 3200 h per year in the most parts of India [3].

Different solar thermal conversion devices are available. Dutta et al. [4–6] have reported energy efficient solar dryer, compact corrugated heat exchanger, different types of air heaters like flat plate, corrugated plate etc. *Garcinia pedunculata*, a locally available medicinal fruit, was dried in an innovative free convection corrugated solar dryer [7]. Sharma et al. [8] studied performance of aluminum can solar air heater. They observed that thermal performance of the aluminum solar air heater was better in terms of thermal efficiency and outlet air temperature. Begum et al. [9] studied parabolic trough collector for purification of drained water. Appropriate design of

solar air heaters (SAHs) is a very crucial aspect for its optimal performance particularly the selection of absorber plate geometry. Ekechukwa and Nortan [10] reported research work on principles of operations, construction, and design of the various SAHs. SAHs may be classified based on the operational modes such as passive, hybrid, and active. Tyagi et al. [11] classified SAHs according to the tracking, non-tracking, with rock bed and PCM materials as the heat storages and the number of glass covers used. Air was heated in various space of duct, and it was directed into the one end of heating applications. It is termed as active SAH. Heat storage may be utilized in an active SAH, and the stored heat is used in the night time. Passive SAHs are rugged and very simple in design, construction and cost are very attractive in contrast to the construction cost of the active SAHs. Air heater may also be classified according to number of air passes; i.e., uni-pass, double-pass and multi-pass SAHs. The air flows in one approach either above or below the absorber plate from air inlet to outlet of the channel in a single pass SAH. While for a double-pass SAH, air flows in two ways that may be either in counter or parallel flow. Air passes above the collector plate support to shrink the top loss to the environment appreciably. At the other hand, side, edge and the bottom losses are reduced by using insulation material of low-thermal conductivity; e.g., wood, glass wool, saw dust etc. Top cover glass should be of low absorptivity and high transmissivity are preferred. Various researchers modified the main components, e.g., absorber plate and configurations of SAHs for analysis [12–15].

Mahmood [17] studied energy, exergy efficiency of a perforated plate solar air heater and a wire mesh cover at Baghdad. The maximum thermal efficiency with 90° bed slope was 63% for glazed and 47% for unglazed SAH. Corresponding exergy efficiencies were 4.8 and 2.3%, respectively. In another study, Mahmood [18] obtained thermal efficiency 86% at an air mass flow rate 0.018 kg/s. Wang et al. [19] performed thermal performance study with a black-coated perforated aluminum collector. At the air mass flow rate of 0.057 kg/s, maximum thermal efficiency was 75%. Shetty et al. [20] experimentally studied performance of a cross flow solar air heater with perforation. Maximum thermal efficiency was 75.55% at Reynolds number 9,000–15,000 at a perforation diameter 8 mm. Promvonge and Skullong [21] studied enhanced heat transfer in a solar receiver heat exchanger with the punched holes. Nusselt number over the flat plate duct increased around 3.91–5.52 times with a substantial friction loss. Skullong et al. [22] studied thermal efficiency in a solar air heater with the perforated-winglet-type vortex. Perforation diameter 1 mm gave the maximum heat transfer and friction factor up to 6.78 and 84.32 times. Khanlari et al. [25] studied experimentally and numerically a perforated baffle solar air heater for drying applications. They observed best instantaneous efficiency 84.30% at an enhanced mass flow rate. Dutta and Goswami [28] studied thermal performance of two different configurations of solar air heater absorber plates. Therefore, the present literature review addresses various researches and developments work on the efficient solar air heaters. Dutta et al. [29, 30] studied thermal performance of corrugated solar air heater. Sharma and Dutta [31] studied corrugated solar air heater for green tea partial drying.

Based on above literature, the objective of present work considers performance analysis of a perforated and flat plate solar air heaters. The finite volume method (FVM) is used to discretize the 3D equations in the turbulent regime, and the effect of radiation is considered. The behavior of the air flow strictly depends on the flow regime. The problem is simulated for the Tezpur University with latitude 26°65′28" N and longitude of 92°79′26" E with an average altitude of 73 m from the sea level. Moreover, solar radiation data for simulation study was considered for the month of November 2018.

2 Methodology

Both the absorber plates had dimensions of $1800 \times 900 \times 1$ mm^3. The distances between the glazing and absorber plate and the bottom and absorber plate were maintained at 40 mm for both the cases. Perforated plate circular holes pitch was 10 mm, and perforation diameter was 1.5 mm accordingly. The geometry of the perforated and solid mild steel solar air heater absorber plates are presented in Fig. 1a, b.

Fig. 1 **a** Perforated plate double pass. **b** Flat plate double pass
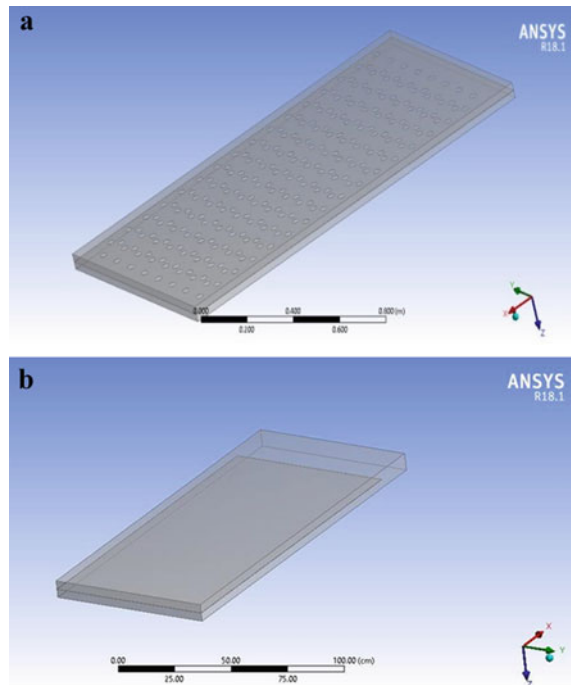
2.1 Governing Mathematical Relationships

The assumptions made for simulation in ANSYS: FLUENT 18.1 are given below. The detailed boundary conditions are presented in Table 1.

i.   The working fluid air flow is assumed as incompressible.
ii. Constant thermal as well as physical properties of the working fluid.
iii. Air flow for the heat transfer study is steady and no slip is at the wall.

The general mathematical equations of continuity, momentum, and energy are given as below [24]:

$$\frac{\partial}{\partial x_i}(\rho v_i) = 0 \tag{1}$$

$$\frac{\partial}{\partial x_j}(\rho v_i v_j) = \left[-\frac{\partial p}{\partial x_i} + \frac{\partial}{\partial x_j}\left[\mu\left(\frac{\partial v_i}{\partial x_j} + \frac{\partial v_j}{\partial x_i} \right) \right] - \frac{2}{3}\mu \frac{\partial v_k}{\partial x_k}\partial_{ij} \right] \tag{2}$$

$$\frac{\partial}{\partial x_j}\left(\rho v_j C_p T - k\frac{\partial T}{\partial x_j} \right) = u_j\frac{\partial p}{\partial x_j} + \mu\left(\left(\frac{\partial v_i}{\partial x_j} + \frac{\partial v_j}{\partial v_i} \right) - \frac{2}{3}\frac{\partial v_k}{\partial x_k}\partial_{ij} \right) \tag{3}$$

The k-ε model was used for study solar air heater performance. The boundary conditions enforced on the perforated and flat plates duct. The local flow was considered turbulent and incompressible. The velocity and pressure boundary conditions were put at the inlet and at the outlet.

The governing mathematical relationship for the standard k-ε model [24] is:

$$\frac{\partial}{\partial x_i}(\rho k v_i) = \frac{\partial}{\partial x_j}\left[\left(\frac{\mu + \mu_t}{\sigma_k} \right)\frac{\partial k}{\partial x_j} \right] + \mu_t\left[\frac{\partial v_i}{\partial x_j} + \frac{\partial v_j}{\partial v_i} \right]\frac{\partial v_i}{\partial x_j} - \rho\varepsilon \tag{4}$$

$$\frac{\partial}{\partial x_i}(\rho\varepsilon v_i) = \frac{\partial}{\partial x_j}\left[\left(\frac{\mu + \mu_t}{\sigma_\varepsilon} \right)\frac{\partial\varepsilon}{\partial x_j} \right]$$
$$+ C_{1\varepsilon}\frac{\varepsilon}{k}\mu_t\left[\frac{\partial v_i}{\partial v_j} + \frac{\partial v_j}{\partial v_i} \right]\frac{\partial v_i}{\partial v_j} - C_{2\varepsilon}\rho\frac{\varepsilon^2}{k} - \alpha\rho\frac{\varepsilon^2}{k} \tag{5}$$

Modeling of turbulent Viscosity:

Table 1 Boundary condition for computation of perforated duct solar air heater

Boundary region	Type of region	flow rate (kg/s)	Pressure (Pa)	Temp. (K)
Inlet	Velocity	0.08	101,315	298
Outlet	Pressure	Out flow	101,305	340
Duct wall	Wall	No slip	–	–
Absorber	Wall	No slip	–	370

Table 2 Grid independency test

Refining levels	Number of elements	Percentage variation of air temperature	Percentage variation pressure drop
1	120,000	3.9	4.9
2	180,000	2.5	3.0
3	320,000	0.54	0.60
4	360,000	0.40	0.55

$$\mu_t = \rho C_\mu \frac{k^2}{\varepsilon} \tag{6}$$

The constants have been reported for the experimental work on fundamental turbulent and shear flows similar to boundary, mixing layers and jets or diminishing isotropic grid turbulence [24]. It applies fine in case of good range of wall-bounded and free shear flows.

2.2 Grid Convergence Test

Grid convergence test is used to define the improvement of the computational results by using uninterruptedly smaller cell sizes. It should converge to the precise results as the mesh become finer. The usual CFD practice is to start with a coarse mesh size and gradually improve it until the deviations perceived in the results are lesser than a predefined acceptable error (Table 2).

For the analysis of the perforated duct, and in order to evaluate the precision of the numerical procedure, the domain for a 2D channel of length 1800 mm, width 900 mm, channel height 40 mm and was tested. To describe the number of elements required, four different meshes were confirmed. The grid independence test was reinforced out in the analysis by accepting dissimilar grid elements as shown in Table 2. The grid individuality tests show that the grids of 320,000 elements assure a satisfactory solution. It is clear that after 320,000 there is not noteworthy percentage difference in appraised parameters.

2.3 Data Reduction

Reynolds, Nusselt numbers, average heat transfer coefficient, hydraulic diameter and pressure drop in the perforated and flat plate ducts are given by Eqs. (7)–(11) [23].

$$R_e = \frac{\rho V D_h}{\mu} \tag{7}$$

$$\overline{Nu} = \frac{\bar{h}D_h}{k} \qquad (8)$$

$$\bar{h} = \frac{Q_u}{A_{\text{duct}}\left(\overline{T}_{\text{wall}} - \overline{T}_{\text{fluid}}\right)} \qquad (9)$$

$$D_h = \frac{4A}{P} \qquad (10)$$

$$\Delta P_{\text{duct}} = \frac{\rho V^2 \, 4fL}{2D_h} \qquad (11)$$

3 Results and Discussion

The perforated and a solid mild steel plates were considered for a double pass solar air heater. The absorbers were designed and investigated for computation of its performance. Keeping all the operating parameters identical for simulation in both the cases, observations were made. Mass flow rate and thermal performance are the most important variables to investigate the thermal efficiency of a solar air heater. Theoretical solar thermal energy potential for the region considered (Tezpur University Campus) throughout the year is depicted in figures below [16]. From Fig. 2, average solar radiation 750 W/m² is considered.

After performing simulation, using ANSYS Fluent version 18.1 the results that are obtained as follows:

For the perforated plate, simulation was done using the S2S radiation model with longitude and latitude as 26°65′28" N and 92°79′26" E. and time zone of +5.5 h. The constants of mathematical modeling are presented in Table 3.

Figure 3 shows temperature distribution in a perforated plate solar air heater. It is clear that for an average solar radiation of 750 W/m², the minimum air temperature 325 K and maximum 335 K near the plate surface. The maximum temperature achievable near perforation (330 K) is less than 335 K because of enhanced heat transfer into the flowing air caused by local turbulence produced.

Since the air velocity through the perforated duct was small, as a result pressure drop from inlet to the outlet is small. Average pressure drop from the inlet to outlet was 0.20 Pa as shown in Fig. 4.

Figure 5 represents overall increasing air temperature from inlet to out of the solar air heater. Maximum air temperature very near to the absorber plate is in the range of 335–338 K. Middle air layer temperatures are around 328 K, and top air layer temperature is around 318 K. Under similar operating conditions, flat plate solar air heater was simulated. The performance results are presented below.

Figure 6 represents temperature distribution in a flat plate solar air heater. It is clear that for an average solar radiation of 750 W/m², the minimum air temperature

Fig. 2 a Maximum solar
radiation intensity on
a horizontal surface (blue),
on a vertical surface (red),
and on a surface
perpendicular to the sunlight
(black). **b** Hourly solar
radiation intensity on
a horizontal surface (blue),
on a vertical surface (red),
and on a surface
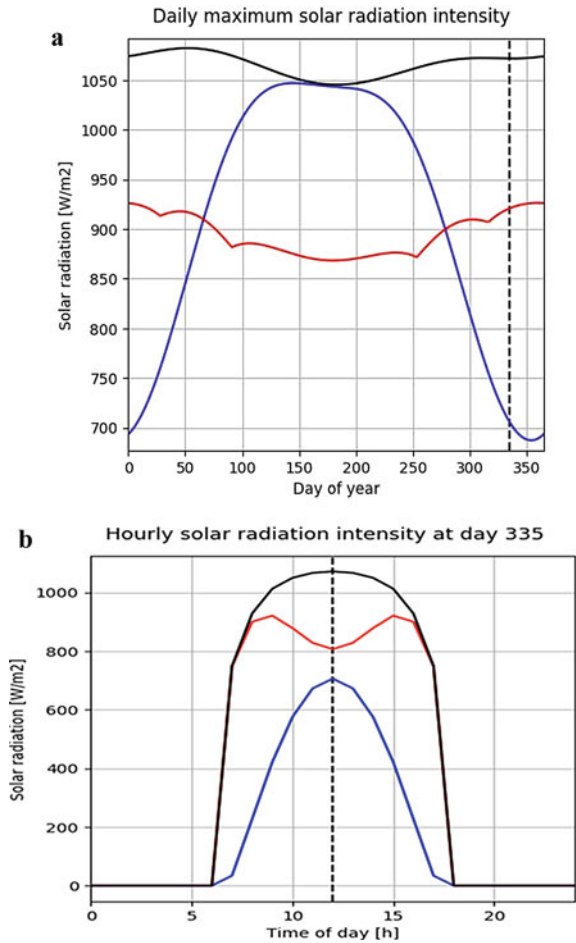perpendicular to the sunlight
(black) on a particular day

Table 3 K-ε model constants

$C_{1\varepsilon}$	C_2	$C_{3\varepsilon}$	σ_ε	σ_k	C_μ
1.42	1.8	1	1.2	1	0.1

305 K and maximum 320 K near the plate surface. Average pressure drop at outlet
is 0.11 Pa as shown in Fig. 7.

Figure 8 represents overall increasing air temperature from inlet to out of the flat
plate solar air heater. The average air temperature just above the absorber plate is
325 K, middle layer is 320 K, and the top average temperature 315 K. There is a
average overall rise in air temperature (318 K) at the outlet.

Figure 9 represents point to point rise in air temperature from inlet to outlet for
both the solar air heaters. For both the air heaters, inlet temperature is almost constant.
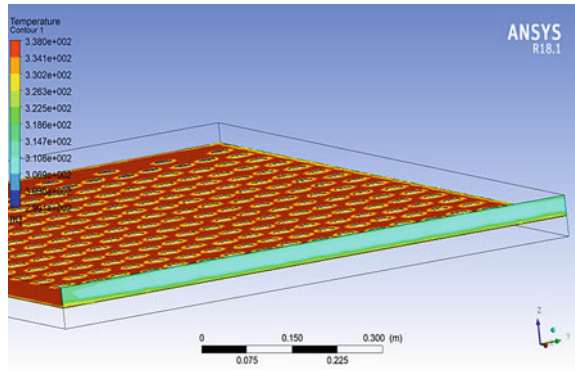
Fig. 3 Temperature distribution from inlet to outlet

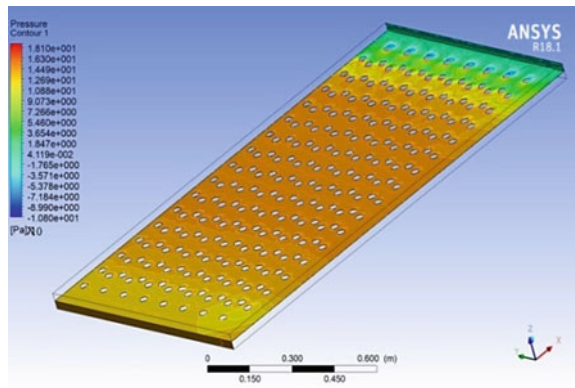**Fig. 4** Pressure distribution from inlet to outlet

Fig. 5 Temperature distribution across the volume of a perforated plate solar air heater
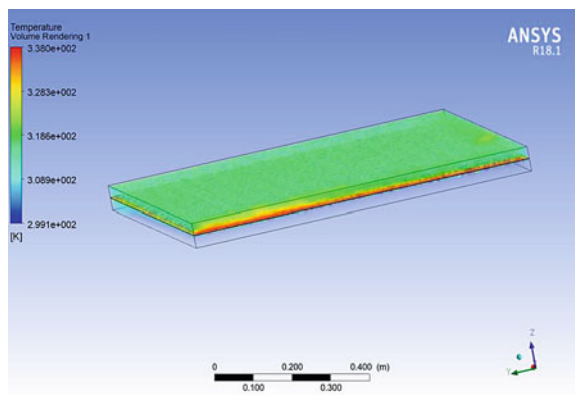
Fig. 6 Temperature
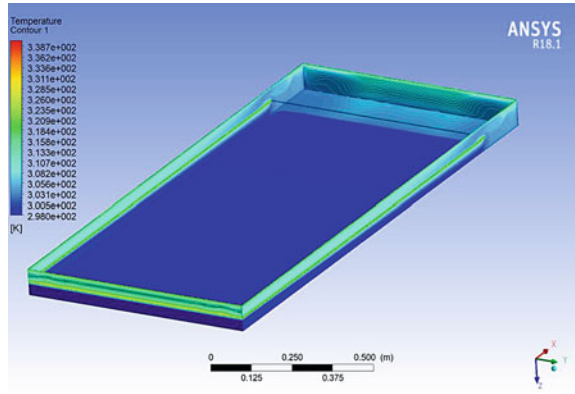distribution across inlet and
outlet (K)

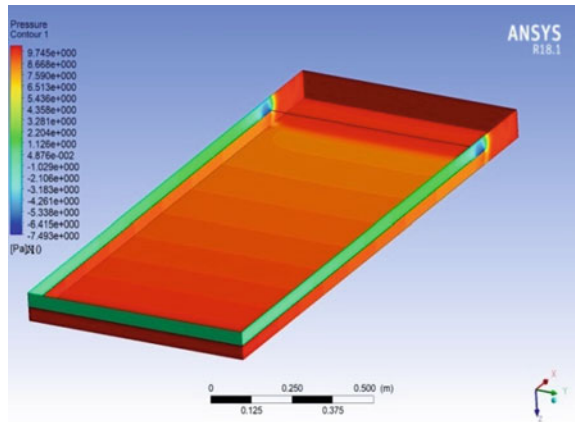**Fig.7** Pressure distribution
at the inlet and outlet

Fig. 8 Temperature
distribution across the
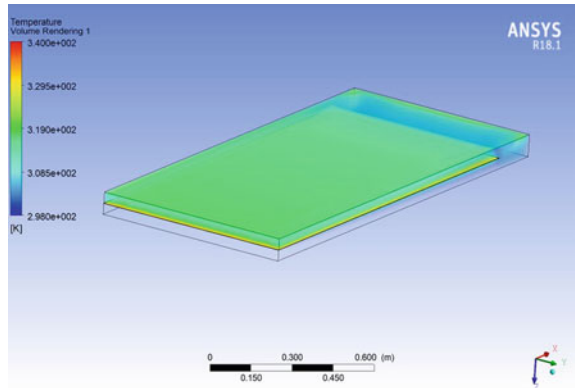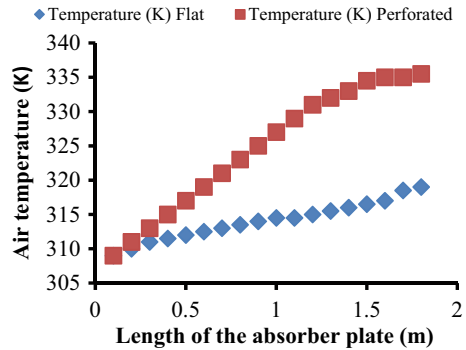volume of flat plate solar air
heater

Fig. 9 Average variation of air temperature from inlet to outlet of flat solar air heater

The average air temperatures increase linearly for both the air heater. The average outlet temperature for the flat air heater was 315 and 335 K for the perforated solar air heater. Hence, there is in an average 20 K more temperature rise for the perforated solar air heater under similar operating conditions. Hence, the perforated double pass solar air heater works satisfactorily than flat double pass solar air heater.

3.1 Validation

The results obtained by, Abuska [9] for energy and exergy analysis of solar air heater have in agreement with present studies. Zheng et al. [26] reported similar temperature rise (average 23 °C) for outlet temperature comparing to inlet temperature. Promvonge et al. [27] also observed enhancement in efficiency for punched delta winglet absorber plate SAH.

4 Conclusion

CFD analysis of a double pass perforated plate solar air heater (SAH) and a flat plate SAH have been performed using Ansys FLUENT 18.1. Both the absorber plates had dimension of $1800 \times 900 \times 1$ mm^3. Finite volume method (FVM) is used to discretize the governing equations. The computational results show that there is a significant improvement in thermal efficiency of a perforated plate double pass comparing to that of a flat plate one for the given mass flow rate of air of 0.08 kg/s.

- For an average solar radiation of 750 W/m^2, the minimum air temperature 325 K and maximum 335 K near the perforated plate surface.
- Average pressure drop at outlet for the perforated plate SAH was 0.20 Pa.
- For the flat plate solar air heater, minimum air temperature 305 K and maximum 325 K near the plate surface.

- Average pressure drop for the flat plate solar air heater at outlet is 0.11 Pa.
- The performance results are in agreement with previously published works.
- Hence, it may be concluded that double pass perforated plate solar air heater absorber plate is a better choice comparing to that of a flat plate from heat transfer performance point of view.
- Energy efficient perforated plate solar air heater may be recommended for development of high-performance indirect type solar dryer for drying of local agricultural produces.

References

1. Yadav, A. S., & Bhagoria, J. L. (2014). A CFD based thermo-hydraulic performance analysis of an artificially roughened solar air heater having equilateral triangular sectioned rib roughness on the absorber plate. *International Journal of Heat. Mass Transfer, 70*, 1016–1039.
2. Bhushan, B., & Singh, R. (2010). A review on methodology of artificial roughness used in duct of solar air heaters. *Energy, 35*, 202–212.
3. Khare, V., Nema, S., & Baredar, P. (2013). Status of solar & wind energy in India. *Renewable and Sustainable Energy Reviews, 27*, 1–10.
4. Dutta, P., Dutta, P. P., & Kalita, P. (2019). Thermohydraulic investigation of different channel height on a corrugated heat exchanger. In *AIP Conference Proceedings*. https://doi.org/10.1063/1.5096502.
5. Dutta, P.P., & Kumar, A. (2017). Development and performance study of solar air heater for solar drying applications. In O. Prakash, A. Kumar (Eds.), *Solar drying technology: Concept, design, testing, modeling, economics and environment* (pp. 579–601). Springer. https://doi.org/10.1007/978-981-10-3833-4_21.
6. Dutta, P. P. (2014). *Prospect of renewable thermal energy in black tea processing in Assam: An investigation for energy resources and technology* (Ph.D. diss). Tezpur University. https://shodhganga.inflibnet.ac.in/handle/10603/37571.
7. Dutta, P., Dutta, P. P., & Kalita, P. (2021). Thermal performance studies for drying of *Garcinia pedunculata* in a free convection corrugated type of solar dryer. *Renewable Energy, 163*, 599–612.
8. Sharma, A., Dutta, P., Goswami, P., Dutta P. P., & Das, H. (2019). Possibility of waste aluminium can for solar air heater through thermal performance studies. In: *Proceeding of International Conference on Waste management towards circular economy from 27/11/2019 to 30/11/2019*. KIIT University.
9. Begum, S. S., Goswami, A. P., Jangid, H., & Dutta, P. P. (2021). Design and modelling of a parabolic trough solar collector. In: B. Kakati, B. R. Phukan, T. Rajbongshi, & D. Bora (Eds.), *Advances in science and technology* (Vol. II, pp. 197–203). Tata Mc Graw Hill.
10. Ekechukwu, O., & Norton, B. (1999). Review on solar energy drying technology. *Energy Conversion and Management, 40*, 615–655.
11. Tyagi, V. V., Panwar, N. L., Rahim, N. A., & Kothari, R. (2012). Review on solar air heating system with and without thermal energy storage system. *Renewable Sustainable Energy Reviews, 16*, 2289–2303.
12. Chamoli, S., Chauhan, R., Thakur, N. S., & Saini, J. S. (2012). A review of the performance of double pass solar air heater. *Renewable Sustainable Energy Review, 16*, 481–492.

13. Singh, S., & Dhiman, P. (2016). Thermal performance of double pass packed bed solar air heaters- a comprehensive reviews. *Renewable able Energy Review, 53*, 1010–1031.

14. Kabeel, A. E., Hamed, M. H., Omara, Z. M., & Kandeal, A. W. (2017). Solar air heaters: Design, configurations, improvement methods, and applications-a detailed review. *Renewable Sustainable Energy Review, 70*, 1189–1206.

15. Abuska, M. (2018). Energy and exergy analysis of SAH having new design absorber plate with conical surface. *Applied Thermal Engineering, 131*, 115–124.

16. https://www.cableizer.com/tools/solar_radiation/ (Dated: 01/12/2018 13:16).

17. Mahmood, A. J. (2019). An experimental study of energy and exergy for glazed and unglazed solar system with perforated absorber plate and wire mesh layers. *International Journal of Renewable Energy Research, 9*(4), 1901–1911.

18. Mahmood, A. J. (2020). Thermal evaluation of a double pass unglazed solar air heater with perforated plate and wire mesh layers. *Sustainability, 12*, 3619. https://doi.org/10.3390/su1209 3619

19. Wang, Y., Boulic, M., Robyn Phipps, R., Plagmann, M., & Cunningham, C. (2020). Experimental performance of solar air collector with a perforated black plate in New Zeland. *Energies, 13*, 1415. https://doi.org/10.3390/en13061415

20. Shetty, S. P., Paineni, A., Kande, M., Madhwesh, N., Sharma, N. Y., & Vasudeva, K. K. (2020). Experimental investigations on a cross flow solar air heater having perforated circular absorber plate for thermal performance augmentation. *Solar Energy, 197*, 254–266.

21. Promvonge, P., & Skullong, S. (2019). Heat transfer augmentation in solar receiver heat exchanger with hole-punched wings. *Applied Thermal Engineering, 155*(5), 59–69.

22. Skullong, S., Promthaisong, P., Promvonge, P., Thianpong, C., & Pimsam, M. (2018). Thermal performance in solar air heater with perforated-winglet-type vortex generator. *Solar Energy, 170*, 1101–1117.

23. Nakhchi, M. E. (2019). Experimental optimization of geometrical parameters on heat transfer and pressure drop inside sinusoidal wavy channels. *Thermal Science and Engineering Progress, 9*, 121–131.

24. Akdag, U., Akcay, S., & Demiral, D. (2017). Heat transfer enhancement with nanofluids under laminar pulsating flow in a trapezoidal-corrugated channel. *Progress in Computational Fluid Dynamics, 17*, 302–312.

25. Khanlari, A., Guler, H. O., Tuncer, A. D., Sirin, C., Bilge, Y. C., Yalmiz, Y., & Gungor, A. (2020). Experimental and numerical study of the effect of integrating plus-shaped perforated baffles to solar air collector in drying application. *Renewable Energy, 145*, 1677–1692.

26. Zheng, W., Li, B., Zhang, H., You, S., Li, Y., & Ye, T. (2016). Thermal characteristics of a glazed transpired solar collector with perforating corrugated plate in cold regions. *Energy, 216*, 781–790.

27. Promvonge, P., & Skullong, S. (2020). Enhanced heat transfer in rectangular duct with punched winglets. *Chinese Journal of Chemical Engineering, 28*, 660–671.

28. Dutta, P. P., & Goswami, P. (2021). A Comparative thermal performance studies between two different configurations of absorber plates in a double pass solar air heater using CFD and experimental analysis. Tata Mc Graw HillIn B. Kakati, B. R. Phukan, T. Rajbongshi, & D. Bora (Eds.), *Advances in science and technology* (Vol. II, pp. 178–183)

29. Dutta, P. P., Kakati, H., Bardalai, M., & Dutta, P. P. (2021). Performance studies with trapezoidal, sinusoidal, and square corrugated aluminium alloy (AlMn1Cu) plate ducts. B. Das, R. Patgiri, S. Bandyopadhaya, V. M. Balas (Eds.), *Modeling, simulation and optimization: Proceedings of CoMSO 2020* (pp. 751–774, Springer, Singapore). https://doi.org/10.1007/978-981-15-9829-6_59.

30. Dutta, P. P., Sharma, D., Das, H., Sharma, A., Dutta, P., & Dutta, P. P. (2021). Computational fluid dynamics and experimental analysis of a corrugated plate duct. *Mathematical Forum, 28*(1), 1–18.

31. Sharma, A., & Dutta, P. P. (2021). Exergy analysis of a solar thermal energy powered tea withering trough. *Materials Today: Proceeding.* https://doi.org/10.1016/j.matpr.2021.06.